BIOCHEMISTRY
including biophysical chemistry & molecular biology

http://pubs.acs.org/doi/abs/10.1021/bi701440z

A reaction center of photosystem II with no peripheral pigments in D2 allows secondary electron transfer in D1[†]

Juan B. Arellano[‡#], Sergio González-Pérez[#], Frantisek Vacha[‖], Thor Bernt Melø[‡], and K. Razi Naqvi[‡*]

[‡]Department of Physics, Norwegian University of Science and Technology. N-7491 Trondheim (Norway).

[#]Instituto de Recursos Naturales y Agrobiología de Salamanca (IRNASA-CSIC), Apdo. 257, 37071 Salamanca, Spain.

[‖]Biological Centre, Academy of Sciences of the Czech Republic and University of South Bohemia, Branišovská 31, 370 05 České Budějovice, Czech Republic.

[*]To whom correspondence should be addressed: Department of Physics, Norwegian University of Science and Technology, N-7491 Trondheim (Norway), Phone: +47-73591853, Fax: +47-73597710, e-mail: razi.naqvi@ntnu.no.

Running title: D1 secondary electron transport in photosystem II

†This work was funded by the Research Council of Norway, the Spanish Ministry of Science and Education (Grant number BFU2004-04914-C02-02), the Czech Ministry of Education, Youth and Sports (Grant numbers MSM6007665808 and AV0Z50510513) and the Spanish and Czech bilateral collaboration program (Grant number CZ2004001).

Abbreviations: AcN, acetonitrile; Car, β-carotene; Chl, Chlorophyll; Chlz, peripheral chlorophyll *a*; Cytb_{559}, cytochrome b_{559}; DM, *n*-dodecyl β-D-maltoside; DmS, doublet-minus-singlet; $D_w \equiv A_a(\lambda) - A_b(\lambda)$, difference spectra, where $w = \lambda/\mathrm{nm}$, and $A_a(\lambda)$ and $A_b(\lambda)$ denote the absorbance (at wavelength λ) after and before photolysis by a cw light source, respectively; FeCy, ferricyanide; LD, linear dichroism; Pheo, pheophytin; PQH_2, plastoquinol; PSII, photosystem II; PVDF, polyvinylidene difluoride; P_{680}, chlorophyll *a* special donor of photosystem II; RC, reaction center; RC-5, five chlorophyll photosystem II reaction center; RC-6, the most active and stable form of the photosystem II reaction center; Q, plastoquinone; SiMo, silicomolybdate; TmS, triplet-minus-singlet; $\Delta A(\lambda;t)$, flash-induced changes in absorbance at wavelength λ and a pump-probe delay time of *t*; $\Delta@d$, abbreviation for $\Delta A(\lambda;t)$ where $d \equiv t/\mathrm{ms} \geq 1$; $C(\lambda)$, absorption spectrum of chlorophyll *a* in 95% acetone; $Z_1(\lambda)$, absorption spectrum of Chlz_{D1} (Chlz in the D1 protein) modeled by red-shifting $C(\lambda)$; $\Sigma(\lambda)$, a smooth fit to the absorption spectrum of $\mathrm{Car}^{+\bullet}$ in AcN; $M(\lambda)$, absorption spectrum of $\mathrm{Car}_{D1}^{+\bullet}$ (the cation of Car in the D1 protein) modeled by blue-shifting $\Sigma(\lambda)$; $\varrho \equiv [\mathrm{Chlz}_{D1}^{+\bullet}]/[\mathrm{Car}_{D1}^{+\bullet}]$, molar ratio $\mathrm{Chlz}_{D1}^{+\bullet} : \mathrm{Car}_{D1}^{+\bullet}$; $\varepsilon_w^{\mathrm{Abb}}$, molar absorption coefficient, at wavelength λ, of the chromophore represented by the abbreviation in the superscript (for $\mathrm{Car}^{+\bullet}$,

$\mathrm{Abb} = \mathrm{Car}+\bullet$; for $\mathrm{Car}_{\mathrm{D1}}^{+\bullet}$, $\mathrm{Abb} = \mathrm{CarD1}+\bullet$; for $\mathrm{Chlz}_{\mathrm{D1}}$, $\mathrm{Abb} = \mathrm{zD1}$; for $\mathrm{Chlz}_{\mathrm{D1}}^{+\bullet}$, $\mathrm{Abb} = \mathrm{zD1}+\bullet$); Δ_w^{Abb}, the value of $\Delta A\left(w\,\mathrm{nm};30\,\mathrm{ms}\right)$ for the chromophore abbreviated in the superscript.

ABSTRACT

A pigment-deficient reaction center of photosystem II (PSII)—with all the core pigments (two molecules of chlorophyll *a* and one of pheophytin *a* in each D protein) but with only one molecule each of peripheral chlorophyll *a* (Chlz) and β-carotene (Car)—has been investigated by pump-probe spectroscopy. The data imply that Car and Chlz are both bound to D1. The absence of Car and Chlz in D2 allows the unprecedented observation of secondary electron transfer in D1 of PSII reaction centers at room temperature. The absorption band of the Car cation in D1 ($Car_{D1}^{+\bullet}$) peaks around 910 nm (as against 990 nm for $Car_{D2}^{+\bullet}$), and its positive hole is shared by $Chlz_{D1}$, whereas $Car_{D2}^{+\bullet}$ can disappear by capturing an electron from $Chlz_{D2}$.

Photosystem II (PSII)[1]—a membrane-embedded pigment-protein complex found in thylakoids of cyanobacteria, algae and higher plants—harnesses the energy of sunlight and catalyses the oxidation of water and the reduction of plastoquinone, releasing molecular oxygen to the atmosphere as a by-product (*1*). The reaction center (RC) of PSII consists of the heterodimer of D1/D2 proteins, the cytochrome b_{559} ($Cyt b_{559}$) subunits PsbE and PsbF and the small subunit named PsbI (*2*); its most active and stable form binds six chlorophyll (Chl) molecules, two pheophytin (Pheo) molecules and two β-carotene (Car) molecules (*3*, *4*). Photo-excitation of the special donor P_{680} of the PSII RC leads to the transfer of an electron to a Pheo molecule. Charge recombination of the resulting ion pair ($P_{680}^{+\bullet}Pheo^{-\bullet}$) is prevented by rapid electron transfer from $Pheo^{-\bullet}$ to the plastoquinone Q_A. After two consecutive steps of reduction of the secondary plastoquinone Q_B, followed by protonation, the plastoquinol (PQH_2) leaves the Q_B site and a new plastoquinone molecule occupies this site. $P_{680}^{+\bullet}$, a species with a high positive redox potential (ca. 1.1 V), is reduced by the tyrosine residue Y_Z (D1-Tyr161) that subsequently oxidizes the Mn cluster, where catalytic water oxidation takes place (*5*). In the event that electron transport from the donor site of PSII is impaired and $P_{680}^{+\bullet}$ is not reduced by the primary electron-donation pathway, a secondary electron-donation pathway comes into effect and protects PSII from oxidative damage induced by

$P_{680}^{+\bullet}$ itself. In this case, Cytb_{559} and oxidizable Chl and Car molecules of RC act as secondary electron donors and reduce $P_{680}^{+\bullet}$ (*6–8*). In isolated membranes or core complexes of PSII, the secondary electron-donation pathway for the reduction of $P_{680}^{+\bullet}$ is unable to compete effectively, at room temperature, with the charge recombination of $P_{680}^{+\bullet}Q_A^{-\bullet}$. In the presence of reduced, high-potential Cytb_{559}, the state Cyt$b_{559}^{+}Q_A^{-}$ is formed preferentially with a yield close to unity after illumination at 77 K (*9*); it has been suggested that in this case Cytb_{559} donates an electron to $P_{680}^{+\bullet}$ via a Car molecule (*7*). In contrast, when Cytb_{559} is preoxidized and is in its low-potential form, electron donation from Chl (again via a Car molecule) takes place (*7*, *10*, *11*); due to the energy barrier for electron donation from Chl to Car, oxidation of Car dominates at temperatures below 20 K, and that of Chl at temperatures above 120 K. A branched pathway, involving Cytb_{559} (which is close to D2), has been put forward; here reduced high-potential Cytb_{559} or Chl (when Cytb_{559} is oxidized) donates an electron to $P_{680}^{+\bullet}$ through an intermediary Car (*7*). However, evidence for the concurrent oxidation of the two nonequivalent Car molecules at 77 K, with different spectroscopic properties, has also been presented (*12*).

The molecular architecture of PSII, as revealed by the 3.0 Å resolution structure (*13*), has led to a better understanding of how secondary electron transfer reactions involving some cofactors in the D2 protein might protect P_{680} in functionally impaired PSII. Due to its favorable location for electron transfer (see Figure 1), the Car in D2 (Car_{D2}) initially donates an electron to $P_{680}^{+\bullet}$, but is rapidly regenerated (at room temperature) through electron transfer from Cytb_{559}, or from the peripheral chlorophyll in D2 ($Chlz_{D2}$) if the former happens to be already oxidized as described above. Electron transfer from the Car in D1 (Car_{D1}) to $P_{680}^{+\bullet}$, less likely when Car_{D2} is present and Cytb_{559} is reduced, could come to the fore in the absence of Car_{D2}; were this to happen, the positive charge would be shared, it has been suggested by Loll and coauthors (*13*, *14*), between Car_{D1} and the peripheral chlorophyll in D1 ($Chlz_{D1}$). The chief obstacle to investigating side electron transport in the D1 protein is the presence of Car_{D2}; we show here that the D2 protein in the pigment-deficient RC (hereafter RC-5) isolated by means of immobilized metal affinity chromatography, is devoid of Car as well as Chlz (*15*), and report the exclusive occurrence of side electron transport in D1 of higher plant PSII RC.

EXPERIMENTAL PROCEDURES

Five-chlorophyll and six-chlorophyll reaction center purification. The five-chlorophyll RC (RC-5) was purified from spinach PSII through Cu-immobilized chromatography as described in (*15*). The RC-5 was eluted from the Cu-immobilized column by adding 5 mM imidazole to the washing buffer, 0.02% *n*-dodecyl β-D-maltoside (DM), 50 mM Mes pH 6.5. The concentrated RC-5 samples were passed through a Superdex 200 size exclusion column (Amersham Pharmacia Biotech., Buckinghamshire, England) equilibrated with 0.02% DM, 20 mM Tris-HCl pH 7.2 (assay buffer) to ensure the RC-5 samples did not contain traces of free pigments or imidazole. In order to compare the absorption spectrum of RC-5 with that of the most active and stable form of the RC containing approximately 6 Chl and 2 Car molecules per 2 Pheo molecules (RC-6), the latter was purified in accordance with the procedure described by Vacha et al. (*15*) and references there in.

Pigment analysis. The pigment stoichiometry of RC-5 and RC-6 was analyzed by HPLC. Pigments were extracted by 80% of acetone (vol/vol), filtered through 0.2 μm polyvinylidene difluoride (PVDF) filter (Whatman plc, Maidstone, UK) and separated on a Zorbax ODS reverse phase column (4.6 x 250 mm, 5 μm) (Agilent

Technologies, Inc., Santa Clara, CA) by isocratic elution with methanol/ethyl acetate, 68:32 (vol/vol), at flow rate 1 ml/min using Waters HPLC system consisting of Pump Controller 600, Delta 600 injection system and a PDA 996 detector (Waters Corporation, Milford, MA). Chromatograms of Chl*a* and Pheo*a* were detected at 663 nm and Car at 450 nm. HPLC was calibrated as described by Vacha et al. (*15*) and the values of 86.9, 49.3 and 135 $mM^{-1}cm^{-1}$ were used for the molar absorption coefficients of Chl*a*, Pheo*a* and Car, respectively, in methanol/ethyl acetate, 68:32 (vol/vol), at the HPLC recording wavelengths. The pigment composition of RC-5 was also examined by means of the spectrum reconstruction method described in (*16*); the advantages of this method are discussed in (*17*). An aliquot of the RC-5 sample was dissolved in acetone and the mixture centrifuged to remove the denatured RC proteins. The final content of water in acetone was 5%. The absorption spectrum of the extracted pigments was recorded by using a commercial spectrophotometer Model UV-1601PC (Shimadzu Scientific Instruments, Inc. Columbia, MD). Chl*a* and β-Car were purchased from Sigma-Aldrich Co. (St. Louis, MO), and Pheo*a* was obtained by acidifying a solution of Chl*a* in acetone (~1 mM HCl). The absorption spectra of the free pigments were recorded in water-acetone (5:95, vol/vol) to match the content of water in the solution of the extracted RC-5 pigment mixture. The molar absorption coefficients

for Chl*a*, Pheo*a* and Car were 81.6, 47.2 and 141 $mM^{-1}cm^{-1}$ in water-acetone (5:95, vol/vol) at 663, 666 and 455 nm, respectively, based on comparative measurements in 100% acetone and published extinction coefficients (*18*).

Transient Absorption spectroscopy. Transient absorption difference spectra of RC-5, $\Delta A(\lambda;t) \equiv A(\lambda;t) - A(\lambda)$ where $A(\lambda)$ and $A(\lambda;t)$ denote the absorbance (at wavelength λ) before and at time t after the firing of the pump source, were recorded by using a home-built multi-channel kinetic spectrometer whose components and operation have been described in (*19*, *20*). The shortest delay was 5 μs; the longest, 30 ms. RC-5 samples were suspended in the assay buffer at an absorbance of 1 at 676 nm in 1-cm cuvette. Anaerobic conditions were reached by directing, 15 min before and during the measurements, a stream of Ar to the surface of the RC-5 sample in the cuvette. When needed, 0.5 mM Silicomolybdate (SiMo) was used as electron acceptor.

RESULTS AND DISCUSSION

Absorption spectra of the isolated RC-5 and RC-6 are shown in Figure 2A. The broad absorption band below 450 nm corresponds to the Soret bands of Chl*a*, Pheo*a* and oxidized Cytb_{559}. The Car absorption band shows a prominent peak at

485 nm and the Q_X band of Pheo*a* appears as a small band at 544 nm. The red region of the spectra is characterized by the prominent Q_y bands of Chl*a* and Pheo*a* that form a single band peaking at 676.0 nm in RC-5 and 675.5 nm in RC-6. The two standard procedures to purify RC-5 and RC-6 are known to yield RC with no plastoquinone in the Q_A (or Q_B) site (data not shown). Based on the assumption that both RC preparations contain 2 Pheo*a* per RC, the spectra were normalized at 544 nm. The normalization shows a decrease in both the absorbance of the Q_y and Soret bands of Chl*a* and the absorbance of the visible band of Car for RC-5 when compared to RC-6. Pigment analysis by HPLC yielded, in the case of RC-5, the average ratio of 5.0±0.1 Chl*a* and 1.2±0.1 Car per 2 Pheo*a*; the corresponding values for RC-6 came out to be 6.2±0.1 and 2.1±0.1, respectively. The outcome of pigment analysis of RC-5 by the spectral reconstruction method (*16*) coincided with the HPLC data; a spectral display of the results appears in Figure 2B. In other words, RC-5 lacks, when compared with RC-6, a Chlz and a Car. On the basis of arguments that will be presented later, we identify the Car in RC-5 as Car_{D1}. As to which of the two molecules of peripheral Chl*a* is lacking in RC-5, it has been suggested that, since $Chlz_{D2}$ is shielded by Cytb_{559} and PsbI subunits of the PSII RC (*21*), the chromatographic procedure used for isolating RC-5 is more likely to

dislodge $Chlz_{D1}$, but our flash photolysis results, presented below, imply otherwise.

Under anaerobic conditions and in the absence of electron acceptors, the difference spectra of RC-5 turned out to be similar to those of RC-6 (*22*). Figure 3 shows two difference spectra at room temperature ($t = 5$ and 30 μs), which have been normalized to the same amplitude at 680 nm. The 30 μs spectrum can be recognized as the triplet-minus-singlet (TmS) spectrum of P_{680}, manifesting the formation of $P_{680}^{\dagger}$ as a result of charge recombination between $P_{680}^{+\bullet}$ and $Phea_{D1}^{-\bullet}$ through the radical pair mechanism; where $P_{680}^{+\bullet}Phea_{D1}^{-\bullet}$ decays with a lifetime of about 45 ns at room temperature (not detected under our experimental conditions) (*23*). Triplet excitation (denoted by the dagger) is believed to be localized mainly on the accessory Chl*a* of P_{680} in D1 (Chl_{D1}) at cryogenic temperature, but in thermal equilibrium (~70:30) with the central special-pair Chl molecules (P_{D1} and P_{D2}) at room temperature (*24*). In the 5 μs spectrum, a small contribution around 530 nm, made by a more short-lived species is apparent; its spectrum, isolated by subtracting the two difference spectra, is shown in the inset of Figure 3. On account of its spectral features and rapid decay, the spectrum in the inset can be identified with $Car^{\dagger}$ (*23*); on the basis of spectral evidence presented later, we will label it as

$Car^{\dagger}_{489}$, and place it in D1. Since $Car^{\dagger}$ can only be populated as a result of triplet-triplet transfer from an adjacent triplet donor, we are led to conclude that the donor in this case must be $Chlz^{\dagger}_{D1}$, which is known to be in van der Waals contact with Car_{D1} (Figure 1). Since the Car_{D2} - $Chlz_{D2}$ separation is appreciably larger, Car_{D2} is expected to be a less efficient quencher of $Chl^{\dagger}$ (*13*), and it would be unreasonable, in the absence of a weighty argument to the contrary, to locate the peripheral pigments of RC-5 in D2.

We pause now to summarize some spectroscopic and structural information about the peripheral pigments and to recall some other data that would prove to be pivotal for the interpretation of our own results. Low temperature linear dichroism (LD) spectroscopy had revealed, before structural data became available, the existence of two spectroscopically distinguishable Car molecules in RC-6: Car_{489} (with an absorption peak at 489 nm), oriented nearly perpendicular to the membrane plane, and Car_{507} (with an absorption peak at 507 nm), lying nearly parallel to the membrane plane (*25*, *26*). On the basis of the available structural information, Car_{489} and Car_{507} can now be identified with Car_{D1} and Car_{D2}, respectively. The absorption spectra of isotropic suspensions of PSII RC, even when recorded at cryogenic temperatures (*27*), are of little help in establishing the identity of the two Car molecules, or for inferring the presence or absence of a Car.

Losi et al. (*28*) did conclude that the Car in RC-5 is Car_{489}, but the evidence does not appear to be compelling. In the absence of LD data on RC-5, we will rely on the difference in the absorption spectra of $\mathrm{Car}_{\mathrm{D1}}^{+\bullet}$ and $\mathrm{Car}_{\mathrm{D2}}^{+\bullet}$.

Charge recombination between $\mathrm{P}_{680}^{+\bullet}$ and $\mathrm{Phe}a_{\mathrm{D1}}^{-\bullet}$, responsible for the formation of $\mathrm{P}_{680}^{\dagger}$, can be prevented by the addition of a suitable electron acceptor, such as SiMo or ferricyanide (FeCy). Low-temperature irradiation of RC-6 under these conditions leads to the formation of a number of species, including $\mathrm{P}_{680}^{+\bullet}$ and Car cation(s), which can be easily investigated by spectroscopic means. Noguchi and coworkers (*29*) conducted a study of RC-6 at 150 K in the presence of FeCy, and reported their results in the form of difference spectra $D_w \equiv A_{\mathrm{a}}(\lambda) - A_{\mathrm{b}}(\lambda)$, where $w = \lambda/\mathrm{nm}$, $A_{\mathrm{a}}(\lambda)$ and $A_{\mathrm{b}}(\lambda)$ denote the absorbance (at wavelength λ) after and before photolysis, respectively. They observed a sharp negative peak at 682 nm, due to bleaching of P_{680}, and a broad, unstructured positive band peaking at 1004 nm; since negative peaks were also seen (at 508, 476 and 440 nm) where Car_{507} (or $\mathrm{Car}_{\mathrm{D2}}$) is known to absorb (*30*), the positive band at 1004 nm was assigned to $\mathrm{Car}_{\mathrm{D2}}$; absorption by a species other than $\mathrm{Car}_{\mathrm{D2}}^{+\bullet}$, particularly $\mathrm{P}_{680}^{+\bullet}$, could not be discerned in the 700–1200 region, and that D_{1004} was nearly equal to $|D_{682}|$. Telfer et al. (*12*) conducted a similar investigation, using SiMo instead of FeCy and Raman

spectroscopy in addition to absorption spectroscopy. They reported that Car_{489} is also depleted "but to a lesser extent (~ 30% of the total carotenoid bleaching)"; they were able to rationalize the excitation profile of the ν_1 mode ($\sim 1490\ cm^{-1}$) by assuming "that the absorption shift [for the two Car cations] is the same as that for their two neutral counterparts—i.e. that $Car_{507}^{+\bullet}$ absorbs at longer wavelengths than $Car_{489}^{+\bullet}$". Since the energy difference between 489 nm and 507 nm corresponds to about $730\ cm^{-1}$ and the absorbance of $Car_{507}^{+\bullet}$ peaks around 990 nm, that of $Car_{489}^{+\bullet}$ would be expected to occur, if one accepts their assumption, at approximately 923 nm. As for $P_{680}^{+\bullet}$, they stressed: "It is of particular interest to note that no detectable bands could be observed at higher frequencies, where carbonyl vibrations of $Chl^{+\bullet}$ species are expected to contribute". That the absorption spectrum of $P_{680}^{+\bullet}$ differs so markedly from that of $Chl^{+\bullet}$ species can be understood, according to Okubo et al. (*31*), by invoking delocalization of the positive charge in a Chl dimer. The stage has now been set for the presentation and interpretation of our own observation.

Flash-induced changes in the absorption spectrum of a RC-5 sample incubated with SiMo are shown in Figure 4. The spectrum at $t = 5\ \mu s$ agrees with the observations of Noguchi and coauthors (*29*): one sees bleaching of P_{680} at 681 nm without any clear indication of a positive signal at wavelengths longer than 700

nm, where $P_{680}^{+\bullet}$ would be expected to absorb if its absorption spectrum bore any resemblance to that of $Chlz^{+\bullet}$, which absorbs weakly in the 820–850 nm region (*8*). As the delay becomes longer ($d \equiv t/\mathrm{ms} \geq 1$), a gradual reduction in the negative signal at 681 nm takes place, accompanied by a growth, at longer wavelengths, of a positive signal, which peaks around 910 nm, and by a negative contribution in the region of absorption by the Car in RC-5. Allowing for the difference in experimental conditions (sample preparation, temperature, acceptor concentration), it is natural to propose that the 910 nm species is $Car_{D1}^{+\bullet}$ (or Car_{489}), and to place the Car in RC-5 in D1. This means that the transient spectra recorded at long delays portray the recovery of the ground state of P_{680} due to electron transfer from Car_{D1} to $P_{680}^{+\bullet}$; as suggested by Loll and co-workers (*13*, *14*), the positive hole will be shared between Car_{D1} and $Chlz_{D1}$. If the broad band in the 700–1000 nm region is indeed a superposition of $Car_{D1}^{+\bullet}$ and $Chlz_{D1}^{+\bullet}$, the negative peak around 680 nm in a *long-delay* spectrum ($\Delta@d, d \geq 1$) must be a superposition of the bleaching signals of P_{680} and $Chlz_{D1}$, which is believed to have its peak absorbance at about 672 nm at room temperature (*32*).

In order to verify the above deduction, we decided to generate $Car^{+\bullet}$ through photo-initiated electron transfer in acetonitrile (AcN), and evaluated the molar

absorption coefficient of $Car^{+\bullet}$ by recording the doublet-minus-singlet (DmS) spectrum of Car (Figure 5). The spectrum of $Car^{+\bullet}$ in AcN, which peaks around 930 nm with $\varepsilon_{930}^{Car+} = 2.2\times10^5\ M^{-1}\ cm^{-1}$, was fitted to a noise-free curve (a sum of gaussians) that will be denoted here as $\Sigma(\lambda)$. Since the band attributed to $Car_{D1}^{+\bullet}$ is slightly blue-shifted with respect to $\Sigma(\lambda)$, it was modeled as $M(\lambda)\equiv\Sigma(\lambda+\lambda_0)$, and λ_0 was found by fitting $M(\lambda)$ to $\overline{\Delta@d}$ (the average of $\Delta@5$, $\Delta@10$, $\Delta@20$, and $\Delta@30$) in the spectral range where $Car_{D1}^{+\bullet}$ is the dominant absorber (880–1000 nm). The difference $M(\lambda)-\Sigma(\lambda)$ is barely above the noise level (with a peak value around 0.001), but its overall shape and location (data not shown) are consistent with the known spectrum of $Chlz_{D1}^{+\bullet}$ (*8*). Adopting the value of $\varepsilon_{815}^{zD1+\bullet} = 10^4\ M^{-1}\ cm^{-1}$ for the peak molar absorption coefficient of $Chlz_{D1}^{+\bullet}$ (*8*), and assuming that $\varepsilon_{910}^{CarD1+\bullet} = 2\times10^5\ M^{-1}\ cm^{-1}$, the value found in AcN, we conclude tentatively that the molar ratio $\varrho\equiv\left[Chlz_{D1}^{+\bullet}\right]/\left[Car_{D1}^{+\bullet}\right]$ is approximately 1.7.

To consolidate the above estimate through an analysis of the bleaching signals around 680 nm in Figure 4, we assumed first that the absorption coefficients of $P_{680}^{+\bullet}$ and $Chlz_{D1}^{+\bullet}$ are negligible in this spectral region, and secondly that the absorption spectrum of $Chlz_{D1}$, which is believed to absorb maximally at 672 nm (*32*), can be approximate by red-shifting the spectrum of Chl*a* in an organic solvent. Each

member of the set $\Delta@d$ was modeled, in the 550–700 nm region, as a superposition of $\Delta A(\lambda;5\,\mu\text{s})$ and $Z_1(\lambda)\equiv C(\lambda-s)$, where $C(\lambda)$ is the absorption spectrum of Chl*a* in 95% acetone and *s* (i.e. the magnitude of the wavelength shift) is chosen so as to bring the peak absorbance of $Z_1(\lambda)$ at 672 nm. The correspondence between each experimental spectrum and its simulation, illustrated by the plots in Figure 6, is sufficiently close to justify placing some confidence in our spectral decomposition. Further support for the decomposition can be derived by comparing $\left|\Delta_{672}^{\text{zD1}}\right|$, the amplitude of the bleaching of ChlzD1, with $\Delta_{910}^{\text{CarD1+}\bullet}$, the absorbance of $\text{Car}_{\text{D1}}^{+\bullet}$. If we take $\varepsilon_{672}^{\text{zD1}}=8\times10^{4}\ \text{M}^{-1}\ \text{s}^{-1}$ for the peak molar absorption coefficient of Chlz_{D1}, we can calculate ϱ by using the relation $\varrho=\left|\left(\Delta_{672}^{\text{zD1}}\varepsilon_{910}^{\text{CarD1+}\bullet}\right)/\left(\Delta_{910}^{\text{CarD1+}\bullet}\varepsilon_{672}^{\text{zD1}}\right)\right|$, and it comes out to be 2.1±0.3, in fair agreement with the crude value inferred earlier. Our two estimates indicate that about a third of the delocalized positive charge between Chlz_{D1} and Car_{D1} resides on the latter molecule. Our analysis of bleaching signal around 680 nm shows that the growth of $\text{Chlz}_{\text{D1}}^{+\bullet}$ and the incomplete recovery of P_{680} parallel the growth of $\text{Car}_{\text{D1}}^{+\bullet}$ which suggests that, at the longest delay, all three cationic species are almost in equilibrium. Equilibrium between Chlz and P_{680}, but in D2, has also been observed

at long delays in RC-6 when using SiMo as electron acceptor (*33*); the difference absorption spectrum displays a clear shoulder at 672 nm and resembles $\Delta@30$.

Our main conclusions may be summed up as follows: the missing pigments in RC-5 are $Chlz_{D2}$ and Car_{D2}; secondary electron transfer in D1, which comes to the fore only when $Chlz_{D2}$ and Car_{D2} are both absent, has been observed for the first time; the absorption spectrum of $Car_{D1}^{+\bullet}$ is blue-shifted with respect to that of $Car_{D2}^{+\bullet}$, and the positive hole is shared among P_{680}, Car_{D1} and $Chlz_{D1}$. Our study has revealed the possibility of an alternative electron transport for $P_{680}^{+\bullet}$, when the side electron transport in D2 is functionally impaired; this secondary electron donation pathway in D1 is expected to occur with low yield in active PSII complexes and, therefore, not likely to play a major role in vivo.

ACKNOWLEDGMENT

We thank Mr. J. J. Martín for technical assistant in reaction center purification.

REFERENCES

1. Barber, J. (2003) Photosystem II: the engine of life, *Q. Rev. Biophys*. *36*, 71–89.

2. Nanba, O., and Satoh, K. (1987) Isolation of a photosystem II reaction center consisting of D-1 and D-2 polypeptides and cytochrome *b*-559, *Proc. Natl. Acad. Sci. U.S.A. 84*, 109–112.

3. Kobayashi, M., Maeda, H., Watanabe, T., Nakane, H., and Satoh, K. (1990) Chlorophyll *a* and β-carotene content in the D1/D2/cytochrome *b*559 reaction center complex from spinach, *FEBS Lett. 260*, 138–140.

4. Gounaris, K., Chapman, D. J., Booth, P., Crystall, B., Giorgi, L. B., Klug, D. R., Porter, G., and Barber, J. (1990) Comparison of the Dl/D2/cytochrome *b*559 reaction centre complex of photosystem two isolated by two different methods, *FEBS Lett. 265*, 88–92.

5. Goussias, C., Boussac, A., and Rutherford, A. W. (2002) Photosystem II and photosynthetic oxidation of water: an overview, *Philos. Trans. R. Soc. London B 357*, 1369–1381; discussion 1419–1420.

6. Stewart, D. H., and Brudvig, G. W. (1998) Cytochrome b_{559} of photosystem II,

Biochim. Biophys. Acta. 1367, 63–87.

7. Faller, P., Pascal, A., and Rutherford, A. W. (2001) β-carotene redox reactions in photosystem II: Electron transfer pathway, *Biochemistry 40*, 6431–6440.

8. Tracewell, C. A., Cua, A., Stewart, D. H., Bocian, D. F., and Brudvig, G. W. (2001) Characterization of carotenoid and chlorophyll photooxidation in photosystem II, *Biochemistry 40*, 193–203.

9. Hillmann, B., and Schlodder, E. (1995) Electron transfer reactions in photosystem II core complexes from *Synechococcus* at low-temperature - difference spectrum of $P680^+ Q_A^-$/P680 Q_A at 77 K, *Biochim. Biophys. Acta 1231*, 76–88.

10. De Paula, J. C., Innes, J. B., and Brudvig, G. W. (1985) Electron transfer in photosystem II at cryogenic temperatures, *Biochemistry 24*, 8114–8120.

11. Hanley, J., Deligiannakis, Y., Pascal, A., Faller, P., and Rutherford, A. W. (1999) Carotenoid oxidation in photosystem II, *Biochemistry 38*, 8189–8195.

12. Telfer, A., Frolov, D., Barber, J., Robert, B., and Pascal, A. (2003) Oxidation of the two β-carotene molecules in the photosystem II reaction center, *Biochemistry 42*, 1008–1015.

13. Loll, B., Kern, J., Saenger, W., Zouni, A., and Biesiadka, J. (2005) Towards complete cofactor arrangement in the 3.0 Å resolution structure of photosystem II, *Nature 438*, 1040–1044.

14. Ishikita, H., Loll, B., Biesiadka, J., Kern, J., Irrgang, K. D., Zouni, A., Saenger, W., and Knapp, E. W. (2007) Function of two β-carotenes near the D1 and D2 proteins in photosystem II dimers, *Biochim. Biophys. Acta 1767*, 79–87.

15. Vacha, F., Joseph, D. M., Durrant, J. R., Telfer, A., Klug, D. R., Porter, G., and Barber, J. (1995) Photochemistry and spectroscopy of a 5-chlorophyll reaction center of photosystem II isolated by using a Cu affinity column, *Proc. Natl. Acad. Sci. U.S.A 92*, 2929–2933.

16. Naqvi, K. R., Melø, T. B., and Raju, B. B. (1997) Assaying the chromophore composition of photosynthetic systems by spectral reconstruction: application to

the light-harvesting complex (LHC II) and the total pigment content of higher plants, *Spectrochim. Acta Part A 53*, 2229–2234.

17. Naqvi, K. R., Hassan, T. H., and Naqvi, Y. A. (2004) Expeditious implementation of two new methods for analyzing the pigment composition of photosynthetic specimens, *Spectrochim. Acta Part A 60*, 2783–2791.

18. Lichtenthaler, H. K. (1987) Chlorophylls and carotenoids: pigments of photosynthetic biomembranes, *Methods Enzymol*. *148*, 350–382.

19. Arellano, J. B., Yousef, Y. A., Melø, T. B., Mohamad, S. B., Cogdell, R. J., and Naqvi, K. R. (2007) Formation and geminate quenching of singlet oxygen in purple bacterial reaction center, *J. Photochem. Photobiol. B 87*, 105–112.

20. Naqvi, K. R., Melø, T. B., Raju, B. B., Javorfi, T., Simidjiev, I., and Garab, G. (1997) Quenching of chlorophyll *a* singlets and triplets by carotenoids in light-harvesting complex of photosystem II: Comparison of aggregates with trimers, *Spectrochim. Acta Part A 53*, 2659–2667.

21. Zehetner, A., Scheer, H., Siffel, P., and Vacha, F. (2002) Photosystem II reaction center with altered pigment composition: reconstitution of a complex containing five chlorophyll *a* per two pheophytin *a* with modified chlorophylls, *Biochim. Biophys. Acta 1556*, 21–28.

22. Durrant, J. R., Giorgi, L. B., Barber, J., Klug, D. R., and Porter, G. (1990) Characterisation of triplet states in isolated photosystem II reaction centers: oxygen quenching as a mechanism for photodamage, *Biochim. Biophys. Acta 1017*, 167–175.

23. Takahashi, Y., Hansson, Ö., Mathis, P., and Satoh, K. (1987) Primary radical pair in the photosystem II reaction center, *Biochim. Biophys. Acta 893*, 49–59.

24. Noguchi, T. (2002) Dual role of triplet localization on the accessory chlorophyll in the photosystem II reaction center: Photoprotection and photodamage of the D1 protein, *Plant Cell Physiol. 43*, 1112–1116.

25. van Dorssen, R. J., Breton, J., Plijter, J. J., Satoh, K., van Gorkom, H. J., and Amesz, J (1987) Spectroscopic properties of the reaction center and of the 47 kDa chlorophyll protein of photosystem II, *Biochim. Biophys. Acta 893*, 267–274.

26. Kwa, S. L. S., Newell, W., R., van Grondelle, and R. Dekker, J. P. (1992) The reaction center of photosystem II studied with polarized fluorescence spectroscopy, *Biochim. Biophys. Acta 1099*, 193–202.

27. Eijckelhoff, C., Vacha, F., van Grondelle, R., Dekker, J. P., and Barber, J. (1997) Spectroscopic characterization of a 5 Chl *a* photosystem II reaction center complex, *Biochim. Biophys. Acta 1318*, 266–274.

28. Losi, A., Yruela, I., Reus, M., Holzwarth, A. R., and Braslavsky, S. E. (2003) Structural changes upon excitation of D1-D2-Cyt b_{559} photosystem II reaction centers depend on the β-carotene content, *Photochem. Photobiol. Sci***.** *2*, 722–729.

29. Noguchi, T., Tomo, T., and Inoue, Y. (1998) Fourier transform infrared study of the cation radical of P680 in the photosystem II reaction center: evidence for charge delocalization on the chlorophyll dimer, *Biochemistry 37*, 13614–13625.

30. Tomo, T., Mimuro, M., Iwaki, M., Kobayashi, M., Itoh, S., and Satoh, K. (1997) Topology of pigments in the isolated photosystem II reaction center studied by selective, *Biochim. Biophys. Acta 1321*, 21–30.

31. Okubo, T., Tomo, T., Sugiura, M., and Noguchi, T. (2007) Perturbation of the structure of P680 and the charge distribution on its radical cation in isolated reaction center complexes of photosystem II as revealed by fourier transform infrared spectroscopy, *Biochemistry 46*, 4390–4397.

32. Kropacheva, T. N., Germano, M., Zucchelli, G., Jennings, R. C., and van Gorkom, H. J. (2005) Circular dichroism of the peripheral chlorophylls in photosystem II reaction centers revealed by electrochemical oxidation, *Biochim. Biophys. Acta 1709*, 119–126.

33. Telfer, A., Durrant, J., and Barber, J. (1990) Transient absorption spectroscopy of the primary electron donor, P680, in the isolated photosystem II reaction center, *Biochim. Biophys. Acta 1018*, 168–172.

FIGURE LEGENDS

FIGURE 1: Pigment arrangement in photosystem II reaction center. Relative locations of pigments, non-haem iron and cytochrome b_{559} in the most active and stable form of reaction center of photosystem II based on the 3.0 Å resolution structure of cyanobacterial photosystem II (PDB code: 2AXT). Relevant π–π system distances for this study ($Chlz_{D1}$-to-Car_{D1}-to-Chl_{D1} and $Chlz_{D2}$-to-Car_{D2}-to-Chl_{D2}) are given in ångströms.

FIGURE 2: (a) Room temperature absorption spectra of the five chlorophyll (solid line) and six chlorophyll (dashed line) reaction centers of photosystem II normalized at the Q_X band of pheophytin *a* at 544 nm. The numbers in nm indicate the peak position of the β-carotene, pheophytin *a* Q_X and chlorophyll *a* (and pheophytin *a*) Q_y bands (b) Spectral fitting, based on the spectrum reconstruction method, of the pigment content of the five chlorophyll reaction center. Absorption spectra of the extracted pigment mixture from the five chlorophyll reaction center (curve 1, solid line), and of pure chlorophyll *a* (curve 2), pheophytin *a* (curve 3) and β-carotene (curve 4) in water:acetone (5:95, vol/vol). Reconstruction spectrum

(curve 5, open circle) fitted by using a least-squares routine to the absorption spectrum of the extracted pigment mixture in the 380-750 nm region.

FIGURE 3: Room temperature photo-induced absorption difference spectra of the five-chlorophyll reaction center of photosystem II under anaerobic conditions at delays of 5 μs (solid line) and 30 μs (dotted line); the two difference spectra are normalized to the same amplitude at 680 nm. Each curve is an average of 120 spectra. Inset, subtraction of the normalized 5 μs and 30 μs difference spectra in the spectral region where the carotenoid singlet ground state and the lowest triplet state absorb.

FIGURE 4: Carotenoid cation formation in the five-chlorophyll photosystem II reaction center at room temperature. Photo-induced absorption difference spectra of the five-chlorophyll reaction center of photosystem II in the presence of 0.5 mM silicomolybdate under anaerobic conditions at the following delays: 5 μs (thick solid line), 1 ms (dashed line), 5 ms (dotted line) and 30 ms (thin solid line). Repetition rate: 5 Hz. Each curve is an average of 60 spectra. Inset, subtraction of the 575 nm normalized 5 μs and 30 ms difference spectra in the absorption region of the carotenoid ground state.

FIGURE 5**:** Doublet-minus-singlet spectrum of β-carotene in acetonitrile. The absorption extinction coefficient of the ground state β-carotene is 140 $mM^{-1}cm^{-1}$ at 450 nm in acetonitrile.

FIGURE 6: Absorption difference spectra (experimental and simulated) of the five-chlorophyll reaction center of spinach photosystem II in the presence of 0.5 mM silicomolybdate under anaerobic conditions. (a) 5 ms delay, $\Delta@5$, and (b) 20 ms delay, $\Delta@20$. Experimental transient absorption difference spectrum (curve 1), linear combination (curve 2) of the transient absorption spectrum at 5 μs, $\Delta A(\lambda;5\,\mu s)$, (curve 3) and the absorption spectrum of $Chlz_{D1}$ (curve 4, obtained by shifting the absorption spectrum of chlorophyll *a* in 95% acetone). For more details, see text.

Figure 1

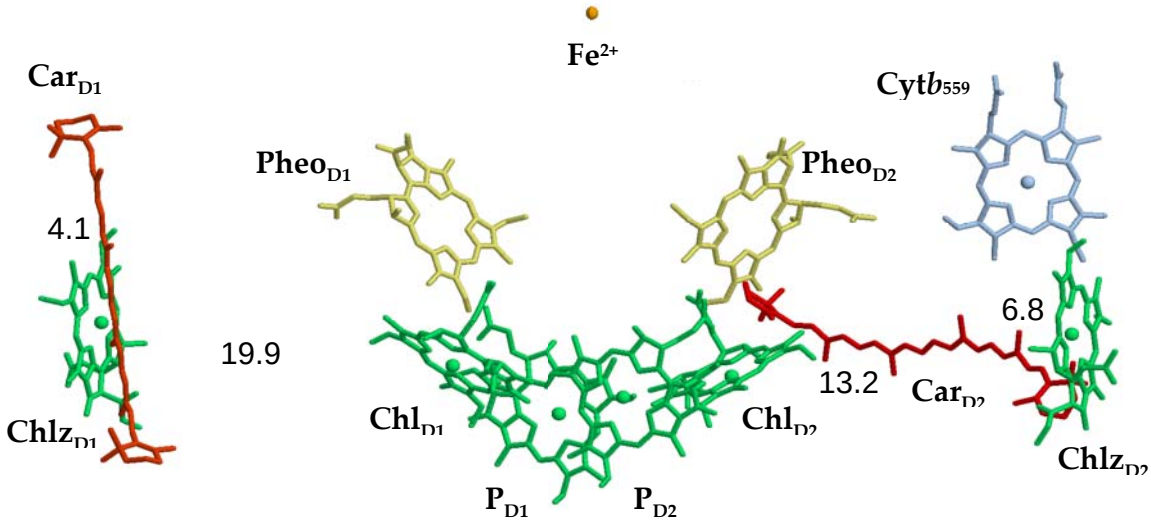
Car$_{D1}$
4.1
Chlz$_{D1}$
19.9
Fe^{2+}
Pheo$_{D1}$
Pheo$_{D2}$
Cyt*b*$_{559}$
6.8
13.2
Car$_{D2}$
Chl$_{D1}$
Chl$_{D2}$
Chlz$_{D2}$
P$_{D1}$
P$_{D2}$

Figure 2

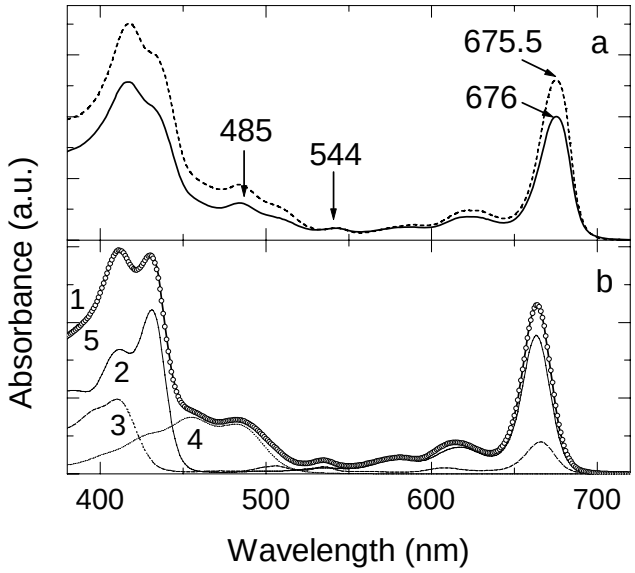
675.5
a
676
485
544
b
1
5
2
3
4
Absorbance (a.u.)
400
500
600
700
Wavelength (nm)

Figure 3

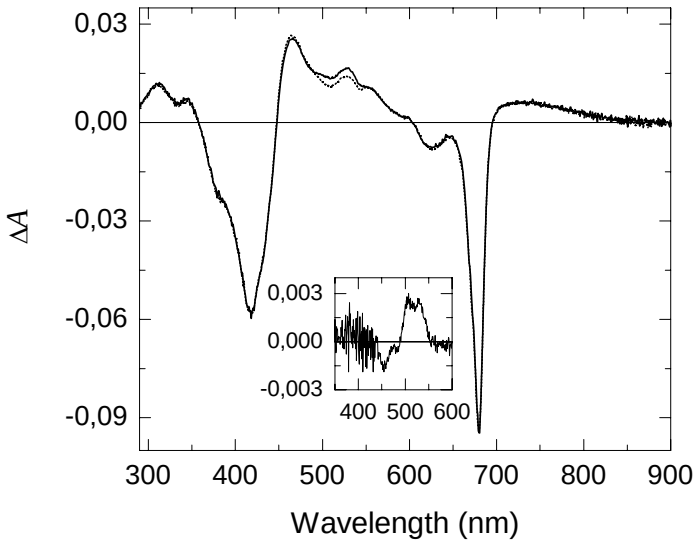
0,03
0,00
-0,03
-0,06
-0,09
ΔA
300
400
500
600
700
800
900
Wavelength (nm)
0,003
0,000
-0,003
400
500
600

Figure 4

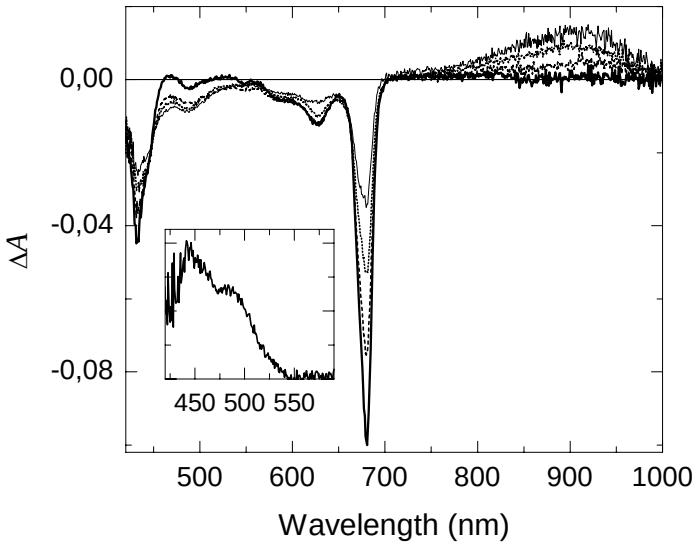
0,00
-0,04
-0,08
ΔA
450 500 550
500
600
700
800
900
1000
Wavelength (nm)

Figure 5.

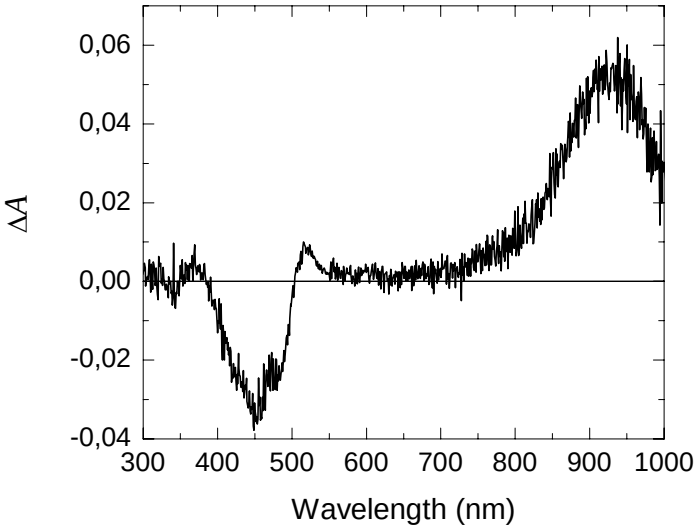
0,06
0,04
0,02
0,00
-0,02
-0,04
ΔA
300
400
500
600
700
800
900
1000
Wavelength (nm)

Figure 6

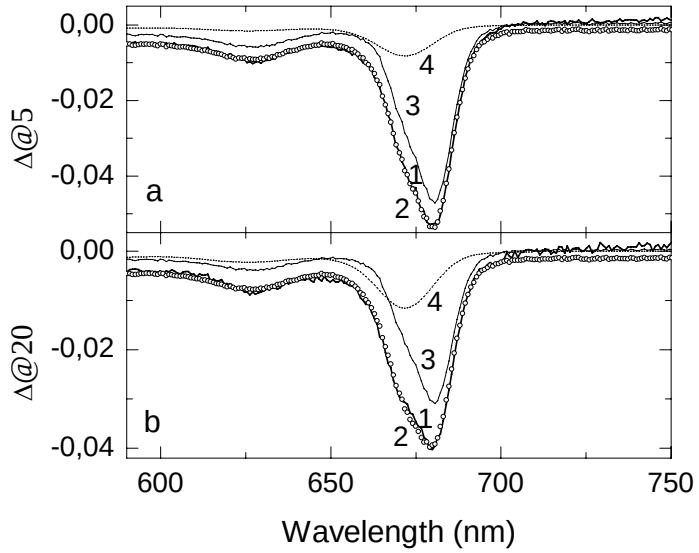
0,00
-0,02
-0,04
Δ@5
a
4
3
1
2
0,00
-0,02
-0,04
Δ@20
b
4
3
1
2
600
650
700
750
Wavelength (nm)

For Table of Contents use Only

A reaction center of photosystem II with no peripheral pigments in D2 allows secondary electron transfer in D1
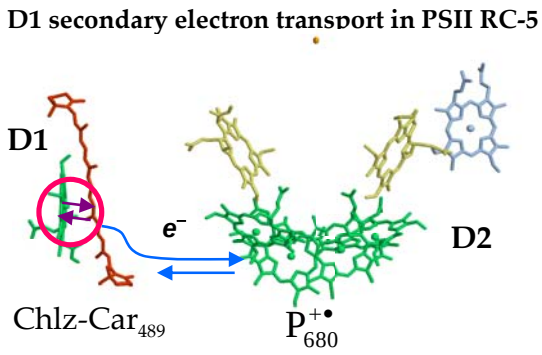
Juan B. Arellano, Sergio González-Pérez, Frantisek Vacha, Thor Bernt Melø, and K. Razi Naqvi